

Computation of mechanical, thermal and electrical properties of CNT/polymer multifunctional nanocomposites using numerical and analytical models

Konstantinos Tserpes^{1,*} and Vasileios Tzatzadakis¹

¹Laboratory of Technology & Strength of Materials, Department of Mechanical Engineering & Aeronautics, University of Patras, Patras, 26500, Greece

Abstract. In the present work, the mechanical, thermal and electrical properties of CNT/polymer nanocomposites are computed using numerical and analytical models as functions of material parameters (CNT aspect ratio, CNT waviness, presence of the interphase) and processing factors (CNT volume fraction, formation of agglomerates and the number and arrangement of CNTs in the agglomerates). The computation is performed using representative unit cells (RUCs) of CNT agglomerates. The RUCs are solved numerically using the FE method and analytically using the Mori-Tanaka method. At the same time, homogenization is applied in the RUCs. The results from the parametric study reveal that the considered parameters and factors govern the reinforcement effectiveness and, under specific combinations, might counterbalance the multifunctionality of nanocomposites.

1 Introduction

Multifunctional composite materials aim to change the way the aircraft industry is designing and manufacturing the load-bearing structures. The concept is that the future materials, which are currently used only for carrying bearing loads, to undertake additional functions [1]. For example, a multifunctional material could be a load-bearing material with excellent thermal and electrical properties providing the structure enhanced resistance to lightning strike and great shielding effectiveness against electromagnetic interference [1]. Nanocomposites (polymers filled by carbon nanotubes (CNTs)) could achieve all these functions due to their excellent mechanical [2-6], thermal [7-9] and electrical [10-16] assigned by the CNTs.

Early experimental studies [6,7-13] have revealed that the properties of CNT/polymer nanocomposites are governed by several material parameters and processing factors and in some cases might be contradictory. Therefore, the development of multifunctional nanocomposites must undergo a proper design and optimization phase which can be performed either by repeated manufacturing trials and physical testing or by virtual testing. It is obvious that the latter method is much more preferable due to the significant benefit in cost and time.

In the present paper, Representative Unit Cell (RUC) models have been developed to predict the mechanical, thermal and electrical properties of CNT/polymer nanocomposites. After proper validation and incorporation of the necessary input data, the models could be easily used for the virtual testing and optimization of nano-enabled multifunctional materials.

2 Analysis

The basic material unit of the present study is a RUC of a CNT agglomerate embedded into the polymeric matrix. Modeling and analysis of the RUC have been performed using the Digimat software.

2.1 Modeling of the CNTs

The RUCs' models have a cubic shape the dimension of which varies according to the CNTs volume fraction, V_f , the number of the embedded CNTs, n , and the volume of the CNTs, V_{CNT} . The dimension a of the RUC is calculated using the formula $a = \left(nV_{CNT} / V_f \right)^{1/3}$. The CNTs have been modelled as straight and curved cylinders. The RUCs have periodic geometry ensuring that the inclusions, which face the limits of the RUC area, are going to be placed as complements inside the RUC in the opposite face. For straight inclusions, the software gives the option to model the interphase between the inclusions and the matrix. Therefore, the presence of the CNT/polymer interphase has been modelled only for straight CNTs.

2.2 Design parameters

In the parametric study, a variety of geometrical characteristics and processing parameters have been considered. These are the CNTs volume fraction, the interphase, the size of the agglomeration (number of CNTs), the CNTs aspect ratio and the CNTs curvature. The value range for these parameters are given in Table 1. The interphase thickness is 9 nm. It is possible for the interphases of one or more CNTs to be interpenetrated to each other. The diameter of the CNTs is 18 nm. The curvature of the CNTs was created automatically by the DIGIMAT software by the setting of the tortuosity factor. Curved inclusions are swept geometries, where the sweep path is a random Bezier curve and the sweep section is a circle. The Bezier curve that is used as sweep path has 11 control points. The first control point is always fixed, while the 10 remaining control points are generated incrementally, each one being placed at a random distance and orientation from the previous one. The tortuosity factor governs the maximum acceptable change in the orientation from one control point to the next. Representative geometries of three RUCs are shown in Fig. 1. The design parameters that were used for the analytical method of Mori Tanaka, were limited to the aspect ratio and the diameter of the CNTs.

Table 1. Parameters and their range.

Parameter	Range
CNT volume fraction	1 ,2 ,3 ,4 ,5%
Interphase	Yes/No
Agglomerate size	20, 30 and 40 CNTs
CNT aspect ratio	20, 40

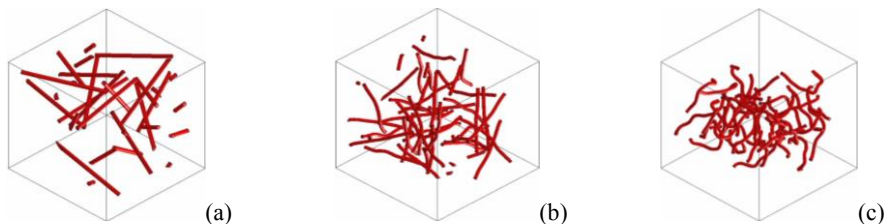


Fig. 1. (a) RUC with straight CNTs, (b) RUC with CNTs of low curvature, (c) RUC with CNTs of high curvature

2.3 FE modeling

The DIGIMAT software has a built-in solver that generates first and second order tetrahedral elements or non-conforming set of bricks elements (voxel mesh). The geometries that were created (both matrix and CNT inclusions) have been meshed with conforming second order tetrahedral elements. A typical FE mesh of a RUC is shown in Fig. 2. In order to calculate the properties of the nanocomposite, the Automatic Properties Evaluation module of the software was used. In addition to the load, (mechanical, electrical and thermal) Periodic Boundary conditions were used for all the faces of the volume element, ensuring the flux of the field variable to be periodic for displacement, temperature and electric potential. Periodic boundary conditions most of the times give better predictions than other sets of boundary conditions but they imply an increased CPU time due to the large set of constraint equations that must be solved.

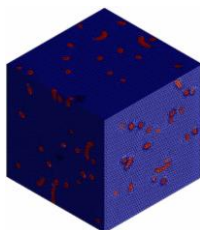


Fig. 2. A typical FE mesh of the RUC

2.4 The Mori-Tanaka (M-T) model

The Mori-Tanaka (M-T) model has been proposed by Mori and Tanaka [17]. The derivation is based on an approximate use of the Eshelby’s solution. It is found that the strain concentration tensor relating the volume average of strain over all inclusions to the mean matrix strain is given by:

$$\mathbf{B}^{\epsilon} = \mathbf{H}^{\epsilon} (I, C_0, C_1) \tag{2}$$

which is exactly the strain concentration tensor of the single inclusion problem. This led Benveniste [18] to give a simple interpretation of the M-T model. Each inclusion in the real RVE behaves as if it was isolated in the real matrix. The body is infinite and subjected to the average matrix strains in the real RVE as the far field (remote) strain. This computational procedure is illustrated in Fig. 3. The M-T model is very successful in predicting the effective properties of two-phase composites. In theory, it is restricted to moderate volume fractions of inclusions (less than 25% say) but in practice it can give good predictions well beyond this range.

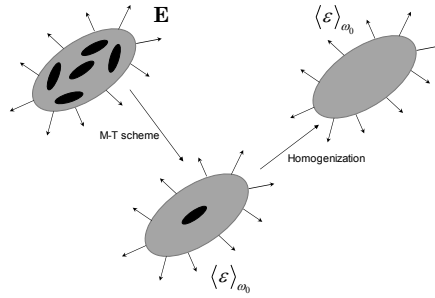


Fig. 3. Schematic illustration of the M-T model

3 Computed results

The material properties that were used in the parametric study are listed in Table 2.

Table 2. Material properties.

Property	Value
CNTs	
Density	1.38E-9 T/mm ³
Young's Modulus	1E+6 MPa
Poisson's Ratio	0.3
Electrical Conductivity	1E+9 A ² S ² /Tmm ³
Thermal Conductivity	6000 W/mK
Specific Heat Capacity	0.181 mJ/TK
Matrix	
Density	1.05E-9 T/mm ³
Young's Modulus	2400 MPa
Poisson's Ratio	0.3
Electrical Conductivity	1E-16 A ² S ² /Tmm ³
Thermal Conductivity	2.16 W/mK
Specific Heat Capacity	0.002 mJ/TK
Interphase	
Density	1.2E-9 T/mm ³
Young's Modulus	1600 MPa
Poisson's Ratio	0.3

3.1 Elastic properties

The elastic moduli E_1 and E_2 , the shear modulus G_{12} and the Poisson's ratio ν_{12} have been computed. Fig. 4 plots the variation of the elastic properties with regards to the number of CNTs, n , with and without the presence of the interphase. It is shown that both parameters do not influence the computed elastic properties of the RUCs. However, the effect of the interphase depends on its thickness and the Young's modulus. Similar findings for the effect of the interphase on the elastic properties of CNT/polymer have been reported in [2,4]. The small deviations obtained for E_2 and ν_{12} are mainly due to the deviation in the geometries of the RUCs, which have been developed using a random process. Similar are the findings for the effect of curvature presented in Fig. 5. The effect of CNTs aspect ratio is presented in the plots of Fig. 6 in combination with the effect of CNTs volume fraction. It is observed that the increase of the elastic properties of the CNT/polymer due to the increase of the CNTs volume fraction is larger for larger aspect ratios. This is an indication

that the reinforcement offered by the CNTs is more effective the larger the length of the CNTs is. From the complete set of results of Figs. 4 to 6, it is also concluded that the presence of CNTs offers an average increase of 20% in the elastic properties of the polymer.

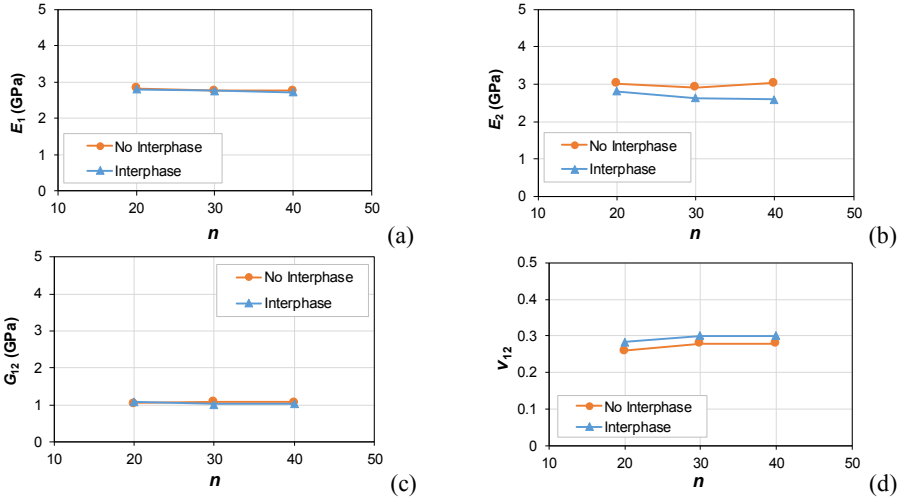


Fig. 4. Numerical elastic properties of the RUC for different number of CNTs with and without interphase.

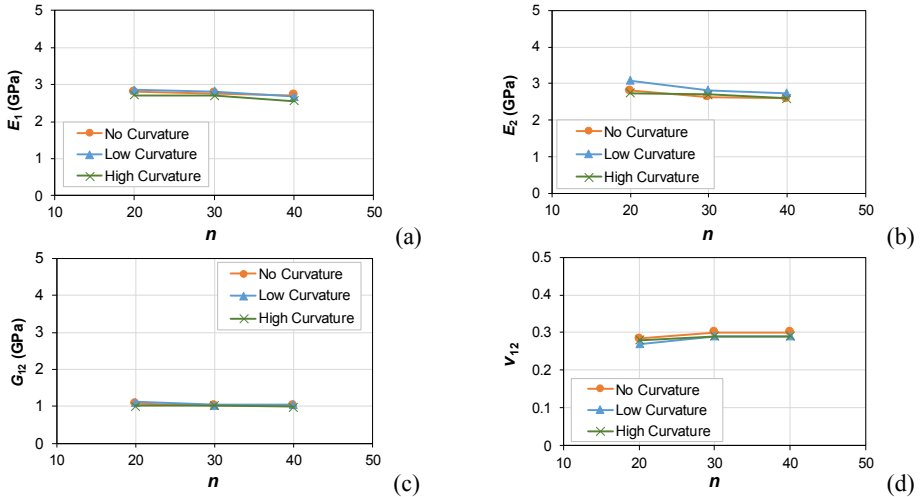


Fig. 5. Numerical elastic properties of the RUC for different number of CNTs of different curvature.

Fig. 7 compares the analytical and numerical computation of E_1 variation with regards to V_{CNT} for the two different CNT aspect ratios. The analytical model captures the effects of both parameters. However, it underestimates E_1 compared to the numerical model and gives a linear variation of E_1 which reveals that it is not capable of considering the geometrical details of the RUCs such as the non-symmetric alignment of the CNTs.

3.2 Electrical conductivity

Electrical conductivity in CNT/polymer nanocomposites is achieved through electrical paths which are either formed by conductive CNTs in contact or are due to the tunneling

effect [14-16]. The distance between the CNTs (inside the non-conductive matrix), which the electrons can move through, has been modelled as 6 nm the maximum.

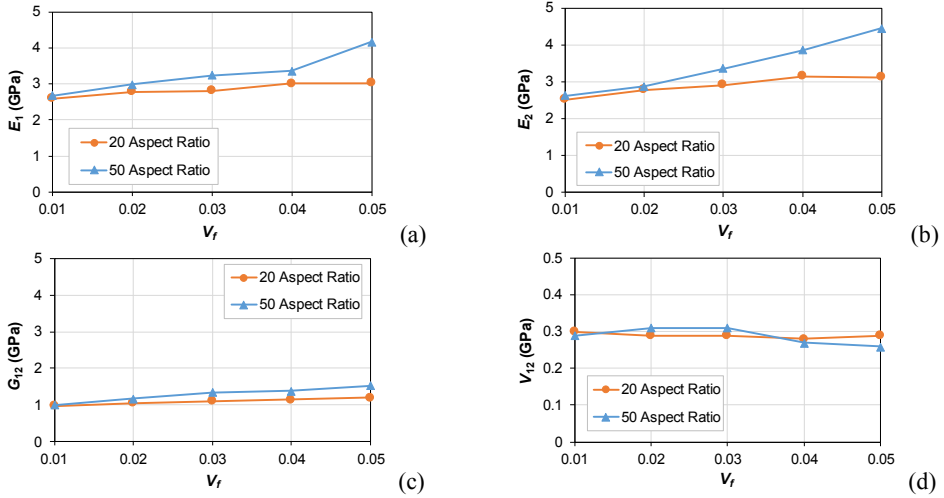


Fig. 6. Numerical elastic properties of the RUC for different CNT volume fraction and aspect ratios.

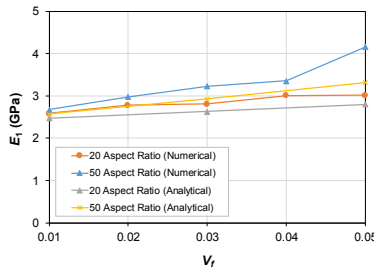


Fig. 7. Numerical vs. analytical longitudinal modulus E_1 of the RUC for different CNT volume fractions and aspect ratios.

In order to assess which parameters and geometric characteristics influence electrical conductivity of nanocomposites, a parametric study has been performed by FE analysis of the RUC and M-T model. The parameters considered in the study are the CNTs volume fraction, the size of the agglomerate (number of CNTs), the CNTs aspect ratio and the CNTs curvature. To the authors' knowledge such a parametric study on electrical conductivity of CNT/polymer nanocomposites does not exist in the literature.

Figs. 8(a-e) plots the numerical electrical conductivity of the RUC for the different parameters considered. It is shown that CNTs volume fraction, aspect ratio, agglomerate size and curvature influence electrical conductivity; the largest effect is coming from the CNTs aspect ratio. In general, there is a synergetic effect of the four parameters which adjusts the formation of small/large, many/few conductive CNT paths into the polymer.

The large effect of CNTs aspect ratio is confirmed by the analytical results shown in Fig. 8(f).

3.3 Thermal conductivity

Fig. 9(a) plots the numerical thermal conductivity of the CNT/polymer with regards to V_{CNT} for straight CNTs, for the two different CNT's aspect ratios and two different sizes of the agglomerates. There is a considerable increase in the thermal conductivity of the neat

polymer (2.16 W/(mK)) due to the addition of the CNTs. The increase is larger for larger V_{CNT} and larger aspect ratios. It starts from the 38% for the case of 20 CNTs, $V_{CNT} = 1\%$, 20 aspect ratio and reaches the 844% for the case of 40 CNTs, $V_{CNT} = 5\%$, 50 aspect ratio. However, it should be noticed that this finding remains to be validated experimentally. The comparison of Figs. 9(a) and 9(b) reveals that there is no effect of CNTs curvature on the computed thermal conductivity of the CNT/polymer. Fig. 9(b) also compares the analytical and numerical computed values of thermal conductivity. The analytical results overestimate the thermal conductivity; however, they capture effectively the effects of V_{CNT} and the aspect ratio giving a linear variation with regards to V_{CNT} .

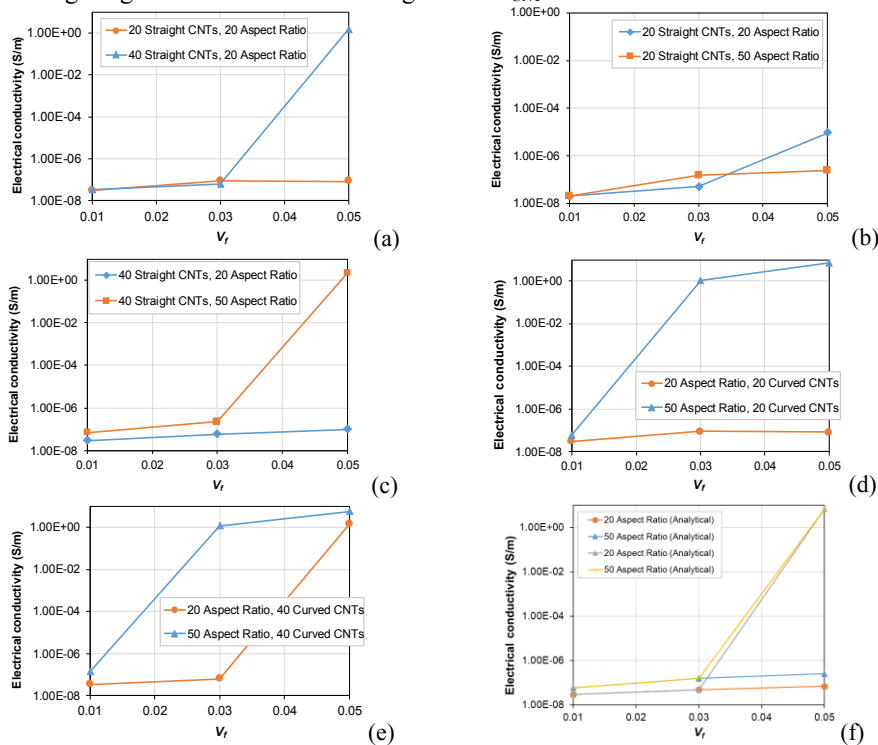


Fig. 8. (a-e) Numerical electrical conductivity of the RUC for different CNT volume fractions, aspect ratio and agglomerate size. (f) Analytical electrical conductivity of the RUC for different CNT volume fractions and aspect ratios.

4 Discussion and conclusions

In the present work, the mechanical, thermal and electrical properties of CNT/polymer multifunctional nanocomposites are computed using numerical and analytical models as functions of material parameters and processing factors. The results of the investigation are summarized in Fig. 10. As expected, the CNTs content has a positive effect on all properties although it is well-known that the higher the CNTs content the larger the CNT agglomerations formed. The same stands for the CNT's aspect ratio. Given the diameter of CNTs is almost fixed, the larger the length of the CNTs, the more effective the reinforcement will be. CNT curvature hinders the mechanical properties of the nanocomposite. Perhaps the most interesting findings is the contradictory effect of the size of agglomerates (number of CNTs) on the mechanical, thermal and electrical properties, which is because the larger the number of CNTs the higher the possibility for the formation

of thermal and electrical networks, as well as the highly synergetic effect of CNTs content, aspect ratio and agglomerate size on the electrical conductivity of the nanocomposite. The results of Fig. 10 can be used as a guideline in the manufacturing of multifunctional nanocomposites and at the same time are a good indication that the present models can be used for the virtual testing and optimization of CNT-enabled multifunctional materials. Regarding the comparison of the analysis methods used, FE analysis of the RUC is more accurate, more practical and capable of modeling/capturing the effects of all parameters. On the other hand, the analytical method can give very fast a first estimation of some of the properties of multifunctional nanocomposites.

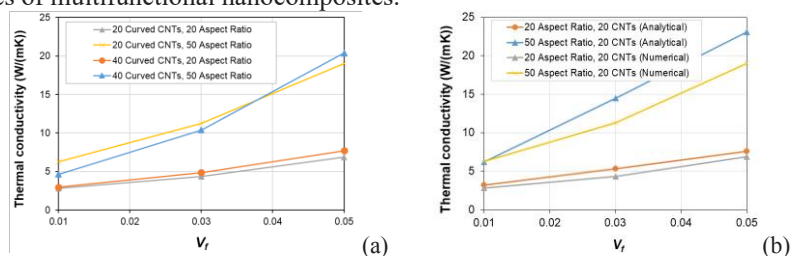


Fig. 9. (a) Numerical thermal conductivity of the RUC for different CNT volume fractions, aspect ratio and agglomerate size. (b) Analytical thermal conductivity of the RUC for different CNT volume fractions and aspect ratios.

	Elastic properties	Electrical conductivity	Thermal conductivity
CNT content	↑	↑	↑
CNT's aspect ratio	↑	↑	↑
CNT curvature	-/↓	↑/-	N/A
Interphase	-	N/A	N/A
Number of CNTs	-/↓	↑	↑

Fig. 10. Summary of the findings of the parametric study.

References

1. A. Ferreira, P. Nóvoa, A. Marques, *Composite Structures*, **151**, 3 (2016).
2. K. Tserpes, A. Chanteli, I. Floros, *Composite Structures*, **168**, 657 (2017).
3. K. Tserpes, et al., *Plastics, Rubber and Composites*, **46**, (2017).
4. K. Tserpes, A. Chanteli, *Composite Structures*, **99**, 366 (2013).
5. A. Chanteli, K. Tserpes, *Composite Structures*, **132**, 1141 (2015).
6. A. Chanteli, K. Tserpes, *Plastics, Rubber and Composites*, **43**, 330 (2014).
7. R. Gulloty et al., *ACS Nano*, **7**, 6 5114 (2013).
8. E. Jackson et al., *Composites Part B: Engineering*, **89**, 362 (2016).
9. Q. Liao, et al., *Scientific Reports*, **5**, 16543 (2015)
10. V. Romano, et al., *AIP Conference Proceedings*, **1981**, 020148 (2018).
11. M. Raimondo, et al., *Composites Part B: Engineering*, **143**, 148 (2015).
12. L. Guadagno, et al., *Composites Part B: Engineering*, **147**, 12 (2018).
13. P Lamberti, et al, *AIP Conference Proceedings* **1981**, 020158 (2018).
14. A. Manta, K. Tserpes, *Composites Part B: Engineering*, **100**, 240 (2016).
15. K. Tserpes, C. Kora, *Computational Materials Science*, **154**, 530 (2018).
16. K. Tserpes, C. Kora, *Aerospace* **5**, 106 (2018).
17. T. Mori, K. Tanaka, *Acta Metall.* **21**, 571 (1973).
18. Y. Benveniste, *Mech. Mater.* **6**, 147 (1987)